Development and Optimization of NOx Reduction Catalysts using Statistical Analysis

Samuel D. Lentz
Honors Thesis for Graduation with Distinction
Submitted: May 22, 2009

The Ohio State University
Department of Chemical and Biomolecular Engineering
140 West 19th Avenue
Columbus, OH 43201

Honors Committee:
Professor Umit S. Ozkan, Advisor
Professor Shang-Tian Yang

Acknowledgements

I want those who have supported and assisted me in this project to know that their efforts and time were deeply appreciated. Starting broadly, I want to thank the Heterogenous Catalysis Research Group, the HCRG, for their friendship and accepting attitude - I felt like I belonged right from the beginning. I want to thank Dr. James Rathman, who taught me the statistical analysis techniques used in this paper as well as taking his personal time to help me and get to know me. I want to thank Meimei Liu for her friendship and her support. We were both new at the research and we made a great team. I especially want to thank Dr. Burcu Mirkelamoglu and Dr. Umit S. Ozkan. Burcu taught me most of what I know in research and helped me more directly than any other person. It would be an understatement to say that without Burcu, I would not have done research or this thesis. Dr. Ozkan believed in me from the beginning and brought me in to the group. Through her (and Burcu) I have received a full-time scholarship, a summer internship, and completed this thesis. I appreciate the time she took to talk to me and encourage me. Most importantly, I want to thank my family and my girlfriend Jennifer Saad. Their support, love, and strength kept me going in the research during some very difficult moments. Lastly, I want to thank God for all that He has done. This project is one of many events that show He has a presence in my life.

Abstract

Increasing regulation and a push towards fuel-efficient automobile engines has driven the development of new NOx emission removal technology for natural gas reciprocating engines and diesel engines. While many technologies have been developed, one of the more promising advances has been the patented dual catalyst approach, which both oxidizes and reduces NOx in the presence of a reducing agent. The system operates by first oxidizing nitrogen monoxide to nitrogen dioxide over a cobalt-based catalyst, and then reducing the nitrogen dioxide to nitrogen over a reducing palladium-based catalyst under the presence of methane (reducing agent). The process is based on findings that it is thermodynamically easier to reduce nitrogen dioxide than nitrogen monoxide and the dual catalyst has shown experimentally to obtain nitrogen yields of close to 90% when operating under simulated exhaust conditions. While the approach has been effective in reducing NOx under dry conditions, the reduction catalyst has shown to deactivate in the presence of water vapor, a common component in engines. This report focuses on the development of new, water-resistant, reduction catalyst formulations that are *active* for NOx reduction with the emphasis on activity. Two pathways were chosen for the synthesis of new catalysts. The first pathway focused on modifying the preparation technique from incipient wetness impregnation to sol-gel technique, which changed the preparation from a physical route to a chemical route. Several levels of alkoxide concentration and nominal sulfuric acid loading were studied to see how these sol-gel parameters impacted surface area, pore volume, and activity. ANOVA and regression modeling were used as a method to determine parameter significance and for optimization work. Results indicated that the nominal sulfate loading heavily impacted the surface area and pore volume with a maximum occurring in the system that may be linked to monolayer surface coverage of sulfate. The alkoxide concentration was less important but the analysis indicated the presence of an interaction effect between the sulfate and alkoxide concentration. XPS data taken on these indicates that samples prepared with an alkoxide

concentration/sulfuric acid ratio (sulfate ratio) of 2 retained the most sulfur after calcination, which was in disagreement with the best-obtained surface area and pore volume. Activity testing ran the new reduction catalysts across a nitrogen dioxide, oxygen, and methane stream to test for nitrogen yield. Results showed that temperature was the primary effect in NOx selective catalytic reduction with alkoxide concentration and sulfate ratio following. Significant interactions were present with a change in one factor affecting others. The sample with a sulfate ratio of 2 and an alkoxide concentration of 1 molar had the best yield though ANOVA showed this point to be a statistical outlier, which added emphasis to the XPS data of maximum sulfur retention. In general, the model showed that increases in alkoxide concentration and increases in the nominal sulfate loading increased NOx reduction activity, though the interactions complicated this system.

The second pathway focused on changing the catalytic support from zirconia to ceria on incipient wetness prepared Pd-based catalysts. Ceria has been shown to be more hydrophobic that zirconia and has been active in other catalyzed reactions. Several catalysts were prepared that varied the palladium loading and sulfate loading on the samples to see how these parameters impacted nitrogen dioxide reduction. Results indicated that all samples failed to show activity and further work is being accomplished to change the formulation.

Table of Contents

LIST OF FIGURES

LIST OF TABLES

Introduction

Nitrogen oxides (NOx) are hazardous air pollutants linked to some of the most pressing environmental and health related problems. The pollution is responsible for the formation of low-lying ozone (smog), acid rain, and increased nitrogen loading in water bodies contributing to accelerated eutrophication. It forms harmful particulates that can penetrate deep into lung tissue causing respiratory problems especially among children and asthmatics. NOx also has the undesired effect of reducing visibility in urban centers and regionally at national parks. The EPA has responded to the threat by issuing increasingly stringent regulations. In addition, there is a growing push towards fuel-efficient vehicles that operate under oxygen-rich conditions such as in diesel and natural gas reciprocating engines. These engines tend to be heavy NOx producers as a result of the excess oxygen. The hazards, increased regulation, and trend towards fuel efficient but NOx-heavy engines has significantly increased the monetary and social costs associated with using NOx producing equipment and have led to a need for the development of effective, efficient, and economical methods to reduce NOx pollution.

Current practice for nitrogen oxide removal is to eliminate emissions at the source, as it is difficult and expensive to separate air pollution once it has entered the atmosphere. The largest sources of NOx are on and off road vehicles and electricity generation plants. While some emissions are produced through combustion of nitrogen species held within fuel (like coal), the majority of NOx gas is produced thermally via high temperature oxidation of nitrogen. Current removal technology has relied largely on selective catalytic reduction (SCR) phenomena using three-way catalysts for mobile applications and ammonia for stationary sources. While both of these aftertreatment technologies are effective within their current applications, they are not able to meet the needs of fuel efficient, lean (oxygen-rich) environments. The three-way catalyst tends to deactivate in lean conditions and ammonia SCR is expensive, is environmentally risky, and

requires a large infrastructure making it impractical for use with smaller units like natural gas reciprocating engines, which are increasing in use. Effectively, it is not possible to solve NOx reduction with a single system. As current NOx aftertreatment applications are insufficient, new technologies are needed that can reduce NOx under lean conditions, while also being affordable and useable for both mobile and stationary sources.

One of the more promising technologies is dual-catalyst selective catalytic reduction. The idea is based upon the competing demand for hydrocarbons (HC) between NOx and oxygen. NO reduction is limited because oxygen is more competitive than NO and can remove methane (the reducing agent) from NOx-SCR by oxidation. However, NO_2 can compete better with oxygen for hydrocarbons as it is already more oxidized. Therefore, it is easier to reduce NO_2 to N_2 than NO to N_2. This reducibility of NO_2 has provided motivation to develop a mixed, oxidation/reduction catalyst that can first oxidize NO to NO_2 by means of an oxidation catalyst and then reduce NO_2 to nitrogen with a reducing agent using a reduction catalyst.

The dual-catalyst approach to NOx reduction has recently been applied with considerable success by the Heterogeneous Catalysis Research Group (HCRG) of the Ohio State University. Members of the HCRG have pursued development of an oxidation and reduction catalyst simultaneously and have developed a mixed catalyst comprised of cobalt on a zirconia support and a palladium catalyst on sulfated zirconia support. The cobalt-based catalyst works to oxidize NO to NO_2 and the palladium-based catalyst then works to reduce NO_2 to nitrogen. The reducing agent used during NO_2 reduction is methane as the process is designed to simulate natural gas reciprocating engine exhaust. This mixed catalyst approach has been patented and is effective in producing nitrogen yields close to 90%, while at the same time oxidizing unburned hydrocarbons and carbon monoxide and utilizing unreacted methane from the engine exhaust to reduce NOx.

Mixing Pd/ZrO_2 and Co/ZrO_2 catalysts has been successful at reducing NOx under dry conditions, but deactivation of the catalyst has occurred in the presence of water vapor, a common component from combustion and SCR in natural gas reciprocating engines. Studies have identified the source of the deactivation to occur in the Pd-based reduction catalyst. Though the effects of water deactivation were somewhat mitigated by increasing the sulfur loading, the current formulation is still inadequate for NOx-SCR in natural gas engines. The next objective for this research, therefore, is the development of new *water resistant* and *active*, reduction catalysts.

The development of water resistant catalysts requires new formulations for the reduction catalyst. These formulations must meet two criteria: (1) New catalysts must be resistant to water vapor deactivation. (2) The new formulations must retain or have improved activity for NOx-SCR. Though both criteria are being pursued simultaneously, the scope of this project focuses on the latter requirement. Two possible formulation pathways have been chosen for study. The first pathway was to change the catalyst preparation technique from incipient wetness impregnation (IWI) to sol-gel method. Sol-gel technique is the process of *chemically* loading an active metal precursor to a support by a hydrolysis reaction. Studies have shown that sol-gel prepared Pd catalysts on sulfated zirconia supports may be more active than the *physical* IWI versions. To understand the potential of sol-gel catalysts on NOx-SCR, several formulations were synthesized that varied the *sulfate ratio* and the *alkoxide precursor concentration* to see how these different preparation parameters impacted activity. Of particular focus was the sulfate loading, as sulfate has shown to increase the acidity, the activity, and the water resistivity of IWI catalysts. In addition, surface area analysis has been completed to see how sulfate and alkoxide concentration affect the catalyst surface area and pore volume. High surface area and pore volume generally correlate to increased active metal dispersion as well as stability in zirconia catalysts.

The second pathway studied the effects of changing the catalytic support from sulfated zirconia to sulfated ceria. Ceria has a high affinity for oxygen and has been shown to be

hydrophobic and thus has potential for being water resistant providing it is also active for NOx-SCR. Six ceria formulations were synthesized (using incipient wetness impregnation) that varied the palladium loading and the sulfur loading to see how the factors impacted activity.

Changing the support, preparation method, and preparation parameters could yield a wide range of results. Past experience has shown it can be somewhat difficult to differentiate what factors (if any) are significant. As an aid, the raw data will be analyzed statistically using Analysis of Variance (ANOVA) and modeled to determine factor significance. Testing using ANOVA may also reveal data outliers and give potential leads for new formulations (optimization).

Literature Review

NOx pollution generally exists in two forms, which are nitrogen monoxide (NO) and nitrogen dioxide (NO_2). The general formula for NO-NO_2 at equilibrium is shown in Equation (1).

$$NO + 1/2O_2 \leftrightarrow NO_2 \quad \textbf{(1)}$$

NOx species tend to be thermodynamically limited with most of the NO_2 decomposing into NO and O_2 at temperatures greater than 800K. NO is thermally more stable than NO_2 due to its high disassociation energy (153.3 kcal/mol), which also results in low NO reduction rates. Without catalysts, it is difficult to reduce NOx even at elevated temperatures [1].

Current aftertreatment technology has relied on three-way catalysts (TWCs) for mobile applications and ammonia SCR for stationary sources. The three-way catalyst typically uses noble metals and ceria to oxidize carbon monoxide and hydrocarbons, while reducing NOx emissions. It is vital that the stoichiometric ratio between fuel and oxygen be maintained as the excess oxygen deactivates the TWC. For more information on TWCs, please consult Burch, who

has provided a comprehensive review on TWCs and the general state of catalysis for mobile applications [2]. Ammonia-SCR has seen widespread use in stationary sources due to its high selectivity of NO in the presence of oxygen, using catalysts such as V_2O_5-WO_3-TiO_2. However, NH_3-SCR has problems due to nitrogen slip, oxidation to hazardous compounds, and storage difficulties especially for on-board applications as those in mobile sources [3].

Zeolite-Based NOx-SCR Catalysts

Considerable research has been done on zeolites and their potential for NOx-SCR. Zeolites are microporous solids that contain very distinct structures. Zeolites generally contain aluminum, silica, and oxygen but can also be doped with cations by ion exchange. Studies have utilized a wide array of zeolites for NO reduction such as ZSM-5, the acidic H-ZSM-5, and ferrierites, among others, and have experimented with even more dopants (Ga, Cu, Fe, In, Pd, Pt, etc). NO reduction with zeolites has been studied for both direct NO reduction and NO reduction with the aid of reducers resulting in varying degrees of success [3-4].

Resasco *et al,* in particular, made several important connections in the fundamental understanding of NOx reduction on zeolites. The group reported that palladium was an active precursor for nitric oxide reduction when reduced with methane in ZSM-5 zeolites. The Pd actively reduces NO but is self-poisoned by the resulting oxygen. Methane mitigates the deactivation of Pd by reacting with the oxygen through oxidation [5]. Additional experiments with acidic Pd/H-ZSM-5 catalysts showed that acid supports are more active for NO reduction than non-acidic supports. It was suggested that the increased acidity caused by the H^+ sites tended to promote the active palladium in some fashion. The work established that both acidity and palladium are needed for high NO conversion. The group concluded that acidity was not exclusive for H-ZMS-5 supports as other types of supports like *sulfated-zirconia* (SZ) were also active for NO reduction, though not as effective as the zeolites [6].

Bell *et al.* furthered the idea of acidity and its link to palladium for NO reduction when studies showed that both acidic H-ZSM-5 and Pd/H-ZSM-5 catalysts were active for NO reduction. The results indicated, however, that the Pd/H-ZSM-5 catalysts were 36 to 88 times more active than H-ZSM-5 catalysts. The work concluded that the increased activity was attributed to Pd^{+2} cations, which are more active than the general Brφnsted acid sites caused by H-ZSM-5 alone [7]. The significance of acid sites was again confirmed by Kung *et al.* where it was suggested that H^+ sites may be more important than zeolite structure. The research also gave evidence for the need of a two-catalyst system as H-ZMS-5 catalysts were highly active for NO_2 to N_2 reduction. It was shown that cobalt could be effective in oxidizing NO to NO_2 and then use H-ZSM-5 to reduce the NO_2 [8].

The high activity for NO_2 reduction may be explained by results from Li and Armor who reported than NO_2 may be a critical intermediate for NO reduction. Thus, it may be easier to reduce NO by first advancing the reaction to NO_2. Li and Armor also reported that water vapor strongly inhibits reaction rates for NO reduction and CH_4 combustion on Co/ferrierite (Co-FER) and may be caused by competitive absorption on the active sites [9]. The effects of water vapor on zeolites were continued where studies showed that Co-ZSM-5 catalysts deactivated under water vapor with a proportional relationship between water vapor levels and reduction activity. Comparison were made between Cu-ZMS-5 and Co-ZSM-5 and showed that while Cu-ZMS-5 deactivation from water vapor was permanent, the Co-ZSM-5 zeolite deactivation was reversible [10]. It is also well known that water vapor tends to cause dealumination in zeolites, and as such, there has been a push to find alternative, non-zeolitic, catalysts.

Non-Zeolites

Current research has largely focused on hydrocarbon selective catalytic reduction (HC-SCR) using non-zeolitic supports. Considerable energy and debate has been focused on metal

oxides, silica, platinum-group metals and the role acidity has on NOx reduction [11-13]. As mentioned previously, Brφnsted acid sites were thought to stabilize Pd^{+2} cations allowing for NO reduction in Pd/H-ZMS-5. The concept of stabilizers was expanded onto non-zeolites when it was confirmed that both sulfated zirconia and tungstated zirconia were indeed effective for Pd-based HC-SCR, and like zeolites, the activity was attributed to stabilization of Pd^{+2} on the support [14-15]. Tungsten doping on zirconia, however, while active, was reported to have lower surface area and a different structural form than that of sulfated zirconia [16].

Sulfated Zirconia Supports

Sulfated zirconia is being heavily researched for its potential in NOx reduction. Zirconia (ZrO_2) is known to be acidic and the addition of sulfate species increases the acidy of the catalyst to the point that some have called sulfated zirconia a superacid [17] for being potentially more acidic than sulfuric acid (H_2SO_4), though this claim has been disputed [18]. Song and Sayari provide an excellent review of SZ and its acidic properties [17]. Resasco *et al* reported that the addition of sulfate onto zirconia for Pd-based NO-SCR was vital for NO reduction as results showed that increasing the wt% of sulfur increased NO conversion [19]. It was hypothesized that sulfate may act as an anchor for the Pd^{+2} cations. Another observed benefit of sulfating ZrO_2 is that studies have shown that sulfate stabilizes the tetragonal phase, crystalline ZrO_2 and tends to have high surface area [20]. Tetragonal zirconia is metastable below high temperatures and prefers the monoclinic phase. Studies have shown, however, that tetragonal form of zirconia is more active than monoclinic form in acid catalyzed reactions [21]. The increased acidity, surface area, and stability caused by sulfate species on sulfated zirconia may be due to the formation of bidentate species (O = S = O) connecting to the zirconia [22-23].

Many studies show that the addition of sulfate to zirconia has a saturation limit with excess SO_4^{-2} present on the catalysts. Resasco *et al.* showed that sulfate loaded onto $Zr(OH)_4$

supports had near linear increasing NO conversion as a function of increased sulfate until about 2.9 wt% SO_4, upon which diminishing returns to conversion were seen [19]. Bautista *et al.* furthered the idea of diminishing returns this by reporting that at ~ 4-wt% SO_4^{-2}, the NO conversion and selectivity began to decrease due to low palladium dispersion [20]. The concept of a maximum in sulfur retention was also observed by Figuéras *et al.* who made SZ catalysts by one-pot sol-gel technique, a different technique than that used by Resasco and Bautista. Evidence from their research suggested that the catalyst formulation with the highest activity was also the sample that had theoretical monolayer coverage of sulfate on the surface [24]. Finally, literature, in general, has suggested that a wide variety of parameters affect the performance of Pd-based sulfated zirconia. Many studies have shown that not only does sulfate loading affect catalyst performance, but the precursor used, the reagent loading, the preparation technique used, and the calcination temperature all impact performance [16,19,20,24-26].

Alternative Supports

While sulfated zirconia has been one of the more studied supports to use for NOx reduction, other metallic supports have shown to be active. One such support is titania (TiO_2). Studies have reported that Pd-based catalysts on titania supports were active for both NO and NO_2 reduction with some formulations depicting significant resistance to oxygen poisoning [27-29]. However, these titania catalysts were deactivated when contacted with SO_2, a common pollutant in emission streams. The SO_2 effects were partially overcome with the additional doping of the galladium, which enhanced the Gd-Pd/TiO_2 catalyst activity and resistance to SO_2 [30]. Nevertheless, Pd/SZ catalysts have shown better resiliency to SO_2 while also retaining high NO conversion [19]. Titania supports have also been used in oxidation catalysts. A cobalt-based TiO_2 catalyst was shown to be effective for oxidation of NO to NO_2 used for the two-catalyst system designed by the HCRG. However, Co/ZrO_2 catalysts still proved to be more active and thermally stable than titania [31].

Ceria supports (CeO_2) are relatively unknown in their applications for NOx reduction. A survey of the literature has shown, however, that ceria has distinctive properties that might aid in NOx research. One of the most useful properties of CeO_2 is its hydrophobicity. In one study, H_2O-TPD's of pure ceria, pure zirconia, and a range of CeO_2-ZrO_2 mixtures showed that ceria was the most hydrophobic and the hydrophilicity increased with increasing levels of zirconia [32]. Ceria has also shown to be active as a catalyst for soot oxidation where Lu *et al.* reported that ceria-based catalysts were more active than ceria-zirconia based ones as ceria had a great number of reducible Ce sites that could take take-in oxygen [33]. It is well known that ceria has a unique capacity to store oxygen.

NOx Reduction Using Dual Oxidation-Reduction Catalysts

From the previous discussion, considerable research has gone into determining a method to reduce nitrogen monoxide into nitrogen with varying success using zeolites, sulfated zirconia, titania, and many more. Now the focus shifts to reduction of nitrogen dioxide to nitrogen (using methane), which is more reducible. Ozkan *et al.* began researching on what eventually became a dual oxidation-reduction catalyst system. The group studied the activity of incipient wetness impregnated Pd/SZ catalysts on NO_2 reduction. Their results came to several conclusions. The group concluded that loading palladium onto SZ using incipient wetness technique had little effect on the surface area of the support. Catalysts pretreated with oxygen from air (calcination) were shown to help stabilize the acidic sulfate groups from leaving the surface up to temperatures of 650°C. Comparisons between NO_2 reduction and NO reduction showed that maximum N_2 yields were obtained when the Pd/SZ reduced NO_2 (57-61%) rather than NO (35%). One unexpected result was the discovery of a side reaction that partially reduced NO_2 back to NO. Further studies showed that the partial reduction was due to a *reduction reaction* and not from decomposition or NO-NO_2 equilibrium effects. With the catalyst and the side reaction working, almost all the NO_2 was converted, though a significant amount of NO was generated, which the

Pd/SZ has more difficulty reducing. The NO produced from the side reaction established the need for an oxidation catalyst to oxidize the produced NO back to NO_2 [34].

With a working reduction catalyst, an appropriate oxidation catalyst was needed to oxidize NO from resulting emission streams and from partial reduction of NO_2. The development of an oxidation catalyst was pursued simultaneously with the reduction research, and it was found that a 10% Co/ZrO_2 catalyst effectively oxidized NO with an equilibrium conversion of greater than 90%. For more information on the development of the oxidation catalyst, please read the dissertation of Dr. Matthew Yung [31]. Many results were obtained by combining the oxidation and reduction catalyst. It was determined that a 0.3 wt% palladium loading was needed for optimized NO_2 reduction and larger palladium loadings tended to aid in combustion of methane rather than reducing NOx. Use of the mixed catalysts for NO reduction showed significantly increased activity (~80%) at the temperature of maximum yield, which was greater than both NO and NO_2 reduction using only the reduction catalyst. Experiments under more realistic exhaust conditions showed that the dual catalyst system was active for the oxidation of CO and higher order hydrocarbons. The benefit of the dual-catalyst approach is that the system can take engine exhaust like methane, reduce NO_2 using the catalyst and methane, and oxidize NO to NO_2 and other undesirables such as CO. A general equation for this system is seen in Equations (2) and (3).

$$NO + \tfrac{1}{2}O_2 \leftrightarrow NO_2 \quad \textbf{(2)}$$

$$2NO_2 + CH_4 \leftrightarrow N_2 + CO_2 + 2H_2O \quad \textbf{(3)}$$

In addition, $NO\text{-}NO_2$ equilibrium is pushed towards NO_2 formation since NO_2 is removed by reduction and the partial reduction of NO_2 is negated by the oxidation catalyst.

The one significant barrier to this system is the deactivation caused by water vapor. It was reported that increasing water vapor decreased N_2 yields and more specifically NO_2 conversion. Experiments suggested that the deactivation of the mixed catalysts was due to competitive absorption of water vapor on the reduction catalyst. The group showed, however, that increasing the sulfur loading onto the zirconia support (by incipient wetness impregnation technique) mitigated some of the deactivation and increased N_2 yields under dry conditions [35].

The catalysts used in the dual-catalyst system were prepared by incipient wetness impregnation technique (IWI), which is the *physical* filling of a porous support by the active metal precursor using an equal pore volume basis. It has been shown that catalysts prepared by sol-gel technique may retain more sulfate groups and may be more active than IWI counterparts. Studies showed that a sol-gel prepared reduction catalyst (Pd/SZ) was active for NO_2 reduction and concluded that the shift from tetragonal zirconia to monoclinic zirconia has less impact on the activity of these specially prepared catalysts [36].

Experimental Methods

Catalyst Synthesis

Catalyst preparation occurred using either incipient wetness technique or sol-gel technique. Incipient wetness impregnation (IWI) is the process of adding an active metal-salt solution to a catalytic support by physical mixing. The volume of solution added to the support should equal the pore volume of the support so that all the liquid fills the pores and does not pool outside the particles. IWI preparation occurred with the ceria catalysts as it is a quicker technique than sol-gel and efficient for screening purposes. First, a predetermined amount of ammonium sulfate was dissolved in water, with a total solution volume equal to the pore volume of the ceria nanopowder used. The solution was then added drop-wise onto ceria nanopowder (<25 nm) and thoroughly mixed and dried overnight at 110°C. After drying, the samples were calcined with air

for 3 hours at 500°C to remove unwanted volatiles and to stabilize the catalyst. Next, palladium chloride was dissolved in a water/hydrochloric acid mixture at a ratio of 2 parts H_2O and 1 part HCl. Once the $PdCl_2$ was dissolved, the solution was added drop-wise in three steps to the sulfated ceria and thoroughly mixed. Between each step, the samples were dried at 110°C for about 30 minutes. The Pd-based sulfated ceria samples were then dried overnight at 110°C and calcined with air for 3 hours at 500°C.

All the zirconia samples were prepared by sol-gel technique. Sol-gel synthesis is useful in that the process is chemical mixing rather than physical. Chemical mixing allows for greater control of parameters and flexibility in developing new and better catalysts. Palladium acetate was dissolved in n-propanol using a stirring bar. The amount of $PdAc_2$ dissolved was such that the final weight of the catalyst would contain 0.3% Pd. Once the palladium was dissolved, 70% zirconium n-propoxide ($Zr(OPr)_4$) in n-propanol was added to the solution and allowed to mix. The $Zr(OPr)_4$ concentration was varied across the samples so that 0.3, 0.6, 1.0, and 1.3 molar were used. Next, sulfuric acid was added to the solution and varied across the samples so that a $Zr(OPr)_4/H_2SO_4$ ratio of 0.5, 1, 2, and 3 were studied. The solution was allowed to mix for 30 minutes to cool any heat given off from the acid addition. Finally, the samples were hydrolyzed with the addition of acetic acid, which was added drop-wise over several hours with a syringe pump. Once the solution gelled, the samples were placed in an oven overnight at 110°C, then crushed with a mortar and pestle, and finally calcined at 600°C for 4 hours.

BET Surface Area and Pore Volume Analysis

The Pd/SZ samples were tested for surface area and pore volume using an ASAP 2010 Micromeritics device. About 200 to 300 mg of a catalyst was placed in a sample tube and sealed. The tube was degassed overnight at 110°C. Once degassed, the sample was reweighed and put into the analysis port and placed in liquid nitrogen. Nitrogen pulses were then sent into the tube

and the instrument measured the resulting pressure, and along with the known weight, calculated the BET specific area and BJH pore volume.

Activity Testing using Steady-state Reaction System

The reaction system used to test NO_2 reduction is shown in Figure 1 and Figure 2. Five mass flow controllers were used that controlled a variety of gases. The 20-Ω furnace was designed in-house and made 0.25 inch diameter stainless steel; the reactor temperature was controlled by a K-type thermocouple connected to an Omega temperature controller. The reactor was loaded with the catalyst and quartz powder so that a total of 400 mg was used. The zirconia catalysts were tested on an equal surface area basis and the ceria samples were tested using an equal mass basis. The quartz powder was mainly a filler so that 400 mg of sample was always tested to keep internal pressure down. The catalyst samples were held by quartz wool in the reactor and placed so that the thermocouple, place inside the reactor, did not contact the sample. The samples were tested over a range of 250-600°C for the zirconia samples and 250-500°C for the ceria samples. Each temperature range occurred at 50°C intervals. The catalysts were tested under a total flow rate of 45 ccm using 1000 ppm NO_2, 3000 ppm CH_4, 10% O_2, and the balance He. After passing through the reactor, part of the gas stream is pumped through an online Varian CP-4900 MicroGC to detect gas compositions. The main stream is sent through a Thermal Environmental 42H Chemiluminescence NOx Analyzer to detect NO, NO_2, and total NOx ppm.

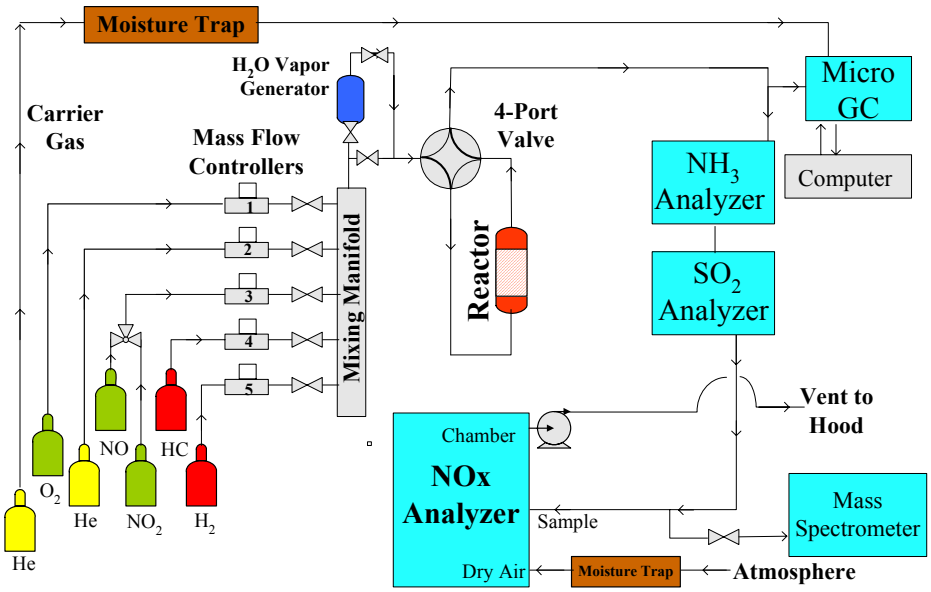

Figure 1: NOx System Schematic

Figure 2: NOx System

Results and Discussion

BET Surface Area and Pore Volume

Eleven Pd/SZ catalysts, prepared by sol-gel technique were tested for specific surface area and pore volume by BET. The samples kept the palladium loading constant at 3 wt% but varied the alkoxide precursor concentration and zirconia n-propoxide/sulfuric acid (mol basis) ratio. The $Zr(OPr)_4/H_2SO_4$ ratio reflects the nominal loading of sulfate into the catalyst with a larger ratio equating to a lower nominal sulfate loading. For this report, the $Zr(OPr)_4/H_2SO_4$ ratio will also be called the sulfate ratio. The alkoxide concentrations tested were 0.3, 0.6, 1, and 1.3 molar. Little is known from literature about the effects of alkoxide concentration on surface area, but it can be intuitively concluded that reduced concentration reduces the hydrolysis rate, which has shown to increase surface area [24]. The $Zr(OPr)_4/H_2SO_4$ ratio was varied from 0.5, 1, 2, and 3. As previously discussed, higher sulfate loadings has been linked to larger surface areas especially when monolayer coverage is obtained [24,25]. High surface areas also equate to better palladium dispersion [20]. The BET specific surface areas obtained from the samples are shown in Table 1 and the pore volumes are shown in Table 2.

Table 1: Surface Area (m^2/g) of 0.3 wt% Pd on Sulfated Zirconia as a Function of Alkoxide Precursor Concentration and $Zr(OPr)_4/H_2SO_4$

Alkoxide Concentration (M)		$Zr(OPr)_4/H_2SO_4$			
		3	**2**	**1**	**0.5**
	0.3	37	69	112	90
	0.6	38	74	109	
	1	48	67		
	1.3	38	60		

Table 2: Pore Volume (m^3/g) of 0.3 wt% Pd on Sulfated Zirconia as a Function of Alkoxide Precursor Concentration and $Zr(OPr)_4/H_2SO_4$

Alkoxide Concentration (M)		$Zr(OPr)_4/H_2SO_4$			
		3	**2**	**1**	**0.5**
	0.3	0.07	0.21	0.34	0.29
	0.6	0.10	0.21	0.38	
	1	0.13	0.23		
	1.3	0.10	0.18		

Observing Tables 1 and Tables 2, it seems that a maximum surface area/pore volume occurs around a $Zr(OPr)_4/H_2SO_4$ ratio of 1. It is unclear if there is a trend in alkoxide concentration or if the points are due to random variation. The maximum surface area occurred at an alkoxide concentration of 0.3 M, whereas the maximum pore volume occurred at a concentration of 0.6 M. For further analysis, the data was statistically analyzed using analysis of variance (ANOVA) at a confidence of 95% (α=0.05). It was assumed that the factors (alkoxide concentration, sulfate ratio) were continuous variables so that a continuous regression model could be developed. The regression model takes on the form of Equation (4):

$$f(x, y) = \beta_0 + \beta_1 x + \beta_2 y + \beta_{12} xy + \text{higher order terms} \quad \textbf{(4)}$$

For better comparison, the factor levels (0.3, 0.6, 1, etc.) were coded so that all levels for variables alkoxide concentration and sulfate ratio would have values between -1 and 1. This coding allows for equivalent scaling of the coefficients for each factor (β_0, β_1, etc). Essentially, coding is eliminating ambiguity caused by each variable having different units in the regression model. The coding formulas shown in Equation (5) and Equation (6) are used to convert between the coded variables and the unit-containing variables for the $Zr(OPr)_4/H_2SO_4$ ratio and alkoxide concentration, respectively.

$$S = \frac{Ratio - 1.75}{1.25} \qquad Zr(OPr)_4/H_2SO_4 \text{ ratio conversion} \quad \textbf{(5)}$$

$$C = \frac{[Alkoxide] - 0.8}{0.5} \qquad \text{Alkoxide Concentration Conversion} \quad \textbf{(6)}$$

The regression model for specific surface area is shown in Equation (7). A summary of the ANOVA results are shown in Table 3 and Figure 3 reports the impact each factor had on specific surface area. All results were held to 95% confidence so any effect that was below 0.05 was statistically significant. Significance is also shown by the '*' symbol next to an effect

probability (P>t or P>F) in Table 3. The regression model developed from these results incorporates statistically significant and borderline statistically significant effects and is valid only over the range of alkoxide concentrations and sulfate ratios studied. The model fits the data to a high degree with an adjusted R^2 value of about 0.985, with a value of 1.000 being an exact fit. Thus, the trends taken from the model fit trends seen in the data. For more detailed results on the analysis of this data, please refer to the attached Appendix. From Equation (7) and Figure 3, it is clear that the sulfate ratio does indeed pass through a maximum as it is cubic form. This maximum, occurring at a ratio of 1, could correspond to the point of monolayer sulfate coverage and this would be consistent with other findings. The alkoxide concentration is also significant, though increases in concentration tended to decrease the surface area. This may be reasonable as increases in concentration may decrease the gelation time in the sample leading to lower surface area. The analysis also indicates a possible sulfate-alkoxide concentration interaction effect; though this effect was borderline significant. The possibility of a sulfate-alkoxide interaction on specific surface area is likely, however, because a power analysis revealed that taking one more BET surface area from one more catalyst sample (of 0.3% Pd/SZ) would have made the interaction significant. The power analysis also reported that there was a 46% chance of type II error, meaning that there was a 46% chance the interaction was significant though it was reported not to be. Observing the coefficients of Equation (7) gives an idea of the magnitude each effect has on surface area. For example the sulfate ratio-cubed effect has a magnitude of 46.77, which is larger than the interaction effect magnitude of 9.45. Thus, the cubic effect is more important than the interaction effect.

$$\textbf{SA } (\textbf{m}^2/\textbf{g}) = 84.81 - 64.71S - 22.79S^2 + 46.77S^3 - 7.19C - 6.60C^2 + 9.45(S*C) \qquad \textbf{(7)}$$

Table 3: ANOVA results of sulfate ratio and alkoxide concentration on BET Surface Area

Response BET Surface Area

Summary of Fit

RSquare	0.993833
RSquare Adj	0.984583
Root Mean Square Error	3.368645
Mean of Response	67.45455
Observations (or Sum Wgts)	11

Analysis of Variance

Source	DF	Sum of Squares	Mean Square	F Ratio
Model	6	7315.3362	1219.22	107.4416
Error	4	45.3911	11.35	Prob > F
C. Total	10	7360.7273		0.0002*

Parameter Estimates

Term	Estimate	Std Error	t Ratio	Prob>|t|
Intercept	84.806296	2.144366	39.55	<.0001*
Sulfate Ratio(0.5,3)	-64.70631	6.265047	-10.33	0.0005*
Sulfate Ratio*Sulfate Ratio	-22.78925	3.62112	-6.29	0.0033*
Sulfate Ratio*Sulfate Ratio*Sulfate Ratio	46.766854	6.38773	7.32	0.0019*
Alkoxide Concentration(0.3,1.3)	-7.190392	2.489208	-2.89	0.0446*
Alkoxide Concentration*Alkoxide Concentration	-6.599311	2.61034	-2.53	0.0648
Alkoxide Concentration*Sulfate Ratio	9.4524161	3.468008	2.73	0.0527

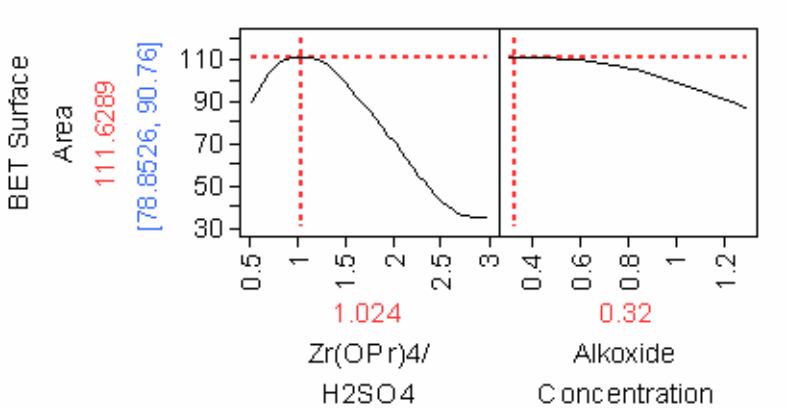

Figure 3: Effect of sulfate ratio and alkoxide concentration on BET surface area (m^2/g)

Using Equation (7), an optimized value for the sulfate ratio and alkoxide concentration can determined by taking the partial derivatives with respect to S and to C and setting the two equations equal to zero. Solving for the two equations and converting from coded variables to unit-containing variables, one can achieve a theoretical maximum specific surface area at a sulfate ratio of 1.02 using 0.32 M $Zr(OPr)_4$. These results are also shown in Figure 3.

The same methodology used to analyze specific surface area was used to analyze specific pore volume. Equation (8) shows the model developed from the reported data. All factors in Equation (8) were significant with the exception of the interaction term between alkoxide concentration and sulfate ratio squared. This factor was borderline significant but included in the model as power analysis showed a 60% chance of type II error with only three more samples needed to detect a difference. The pore volume results are similar to the BET surface area in that the pore volume is heavily influenced by the $Zr(OPr)_4/H_2SO_4$ ratio, which is the nominal sulfate loading. Pore volume also goes through a maximum being cubic form. The trends for pore volume versus each factor are shown in Figure 4. An optimum value for pore volume based off this data trend is about 0.91 $Zr(OPr)_4/H_2SO_4$ with 0.86 M $Zr(OPr)_4$.

$$\textbf{PV } (\textbf{m}^3/\textbf{g}) = 0.28 - 0.26S - 0.05S^2 + 0.14S^3 - 0.03C^2 + 0.02(C*S^2) \quad \textbf{(8)}$$

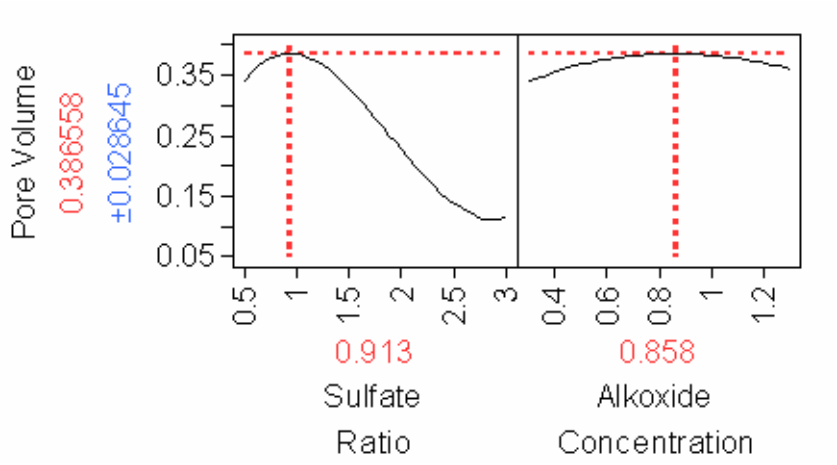

Figure 4: Effect of sulfate ratio and alkoxide concentration on specific pore volume (m^2/g)

Comparing the trends seen between the factors and surface area and pore volume, it seems that the primary difference is caused by the effects of different alkoxide concentrations. The optimized sulfate ratios of 1.02 and 0.91 are relatively similar with a percent difference of 11%, which may be caused from minor effects and/or random variation. The alkoxide concentration, however, has a percent difference of 63%. In general, the specific surface area decreased as a result of increased alkoxide concentration, until a high sulfate ratio (low sulfur loading) of 2 to 3 counteracted some of this trend because of the sulfate ratio-alkoxide concentration interaction (see Equation 7). For pore volume, the alkoxide concentration tends to maximize pore volume around 0.85 M and decrease in either direction. Summarizing these effects, it appears that the sulfate ratio impacts the surface area and pore volume in relatively the same way. There appears to be a maximum around a ratio of 1, which may correspond to monolayer coverage of sulfate on the surface. Alkoxide concentration seems to interact with surface area and pore volume in different ways with high surface area corresponding to decreased concentration and high pore volume going through a maximum around 0.86 M. It is possible the lower alkoxide concentration is actually representing the effect of a slower hydrolysis rate, which is altering the catalyst structure. The calcination temperature may impact these effects as well. There also appears to be the presence of a sulfate ratio-alkoxide concentration interaction effect where changes in one parameter affect the other. Most notably this occurs at low sulfate levels (high ratio) where the decreasing alkoxide effect for surface area changes to a maxima effect; at high enough sulfate ratio some increase in concentration level improves surface area. The pore volume had a squared interaction in sulfate ratio, which was different from surface area. It is unclear how alkoxide concentration and the nominal sulfate loading interact, but may be a point worth investigating. Overall, the $Zr(OPr)_4/H_2SO_4$ ratio is the dominating effect for both surface area and pore volume over these ranges and effects studied.

Comparing Sulfur Retention with Nominal Sulfate Loading

The sulfate ratio effect on surface area and pore volume, while significant, was only a nominal loading. It is well known that many effects impact the true loading and retention of sulfate on the surface (see literature review). To determine if the retained sulfur impacted the surface area and pore volume in the same manner as the nominal $Zr(OPr)_4/H_2SO_4$ ratio, XPS data of the eleven samples was obtained by the generosity of other team members in the HCRG. This data was used to estimate the retained sulfur in the samples after calcination at 700°C for 4 hours. A comparison between the nominal and actual loadings is shown in Figure 5 and the results show that there is a discrepancy between the sulfate ratio and the retention rate of sulfur on the catalyst. The largest surface areas occurred around a nominal sulfate ratio of 1 whereas the samples with greatest sulfur retention occurred at nominal sulfate ratios of 2. A Tukey HSD test was used on the sulfur retention samples to see if the means of the samples were statistically different from one another. The results gave evidence that a $Zr(OPr)_4/H_2SO_4$ ratio of 2 is statistically different from samples with ratios of 1 and 0.5 and a ratio of 3 was statistically different from the ratio of 0.5. In addition, variations in alkoxide concentration were shown to be not significant for sulfur retention over the range studied. A power analysis reported that a total of 62 samples would be needed to determine concentration significance, which is not practical. This failure to be significant is an interesting result as it suggests alkoxide concentration minimally affects the loss of sulfur on the sample. These results also imply that the final retention of sulfur on the sample may not impact the surface area and pore volume of the sample in the way the initial sulfur loadings and alkoxide concentration do. Perhaps the nominal loading and alkoxide concentration has much to do with the initial crystal structure of the catalyst, which is further impacted upon calcination.

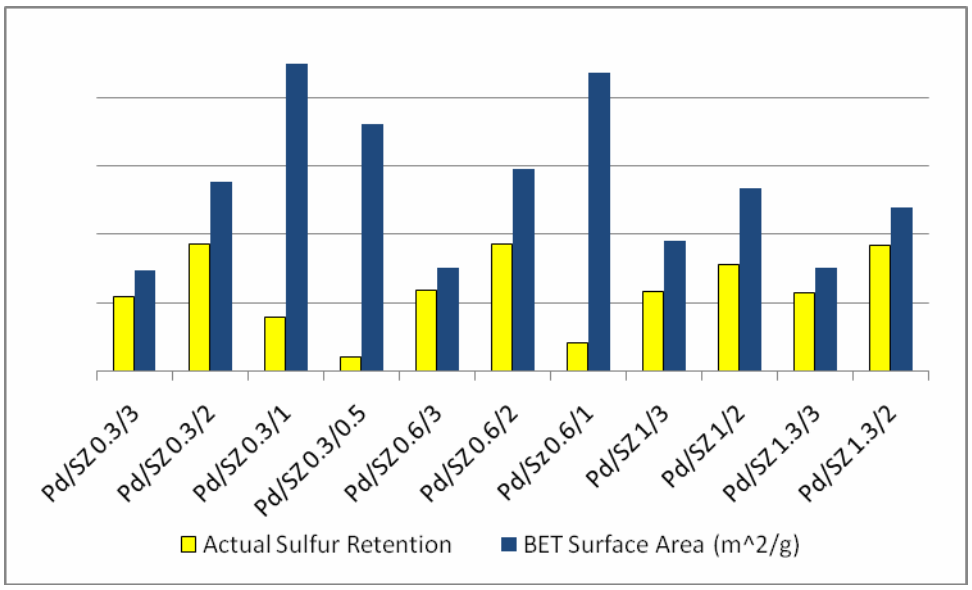

Figure 5: Comparison between actual sulfate retention (%) after calcination at 700°C for 4 hours and sulfate ratio shown through BET surface area (m^2/g). Actual sulfate retention taken from XPS data courtesy of HCRG

Activity Testing of Sol-gel Pd/SZ Catalysts

A total of 14 Pd/SZ catalysts were tested for NO_2 reduction to determine the activity of the samples for producing N_2. The catalysts all used 0.3% palladium but varied the alkoxide concentration and $Zr(OPr)_4/H_2SO_4$ ratio in same manner as the surface area and pore volume samples. Table 3 lists the experiments performed including the number of replicates per sample. Each catalyst was tested within a temperature range of 250-600°C at 50°C intervals over 3000 ppm CH_4, 1000 ppm NO_2, 10% O_2, and the balance He (total flow was 45 ccm). Figure 6 reports on the nitrogen yield as a function of temperatre for a single sample at each level studied. Peak activity generally occurred between 450-500°C, which was expected. The only exceptions were catalysts prepared with 0.3 M $Zr(OPr)_4$ and using low sulfate loadings (ratio of 2 and 3). The peak activity seemed to occur around the catalyst sample with 1 M alkoxide concentration using a sulfate ratio of 2. This catalyst is the 'standard' one used previously by the HCRG. The sample using 1.3 M $Zr(OPr)_4$ with a sulfate ratio of 3 was the next best sample. Observing the data it is

clear that activation temperature is the dominant effect for activation, which is expected. What it is not clear from Figure 6, is how sulfur and alkoxide concentration impact the nitrogen yield.

Table 3: Experimental Design for NO_2-SCR Activity Testing displaying factor levels and number of trials run per level.

$Zr(OPr)_4$ Concentration [M]	$Zr(OPr)_4/H_2SO_4$				
		3	**2**	**1**	**0.5**
	0.3	1	2	*rejected sample*	1
	0.6	1	1	1	
	1	1	1		
	1.3	2	1, *rejected sample*		

Indicates bad sample not used in analysis

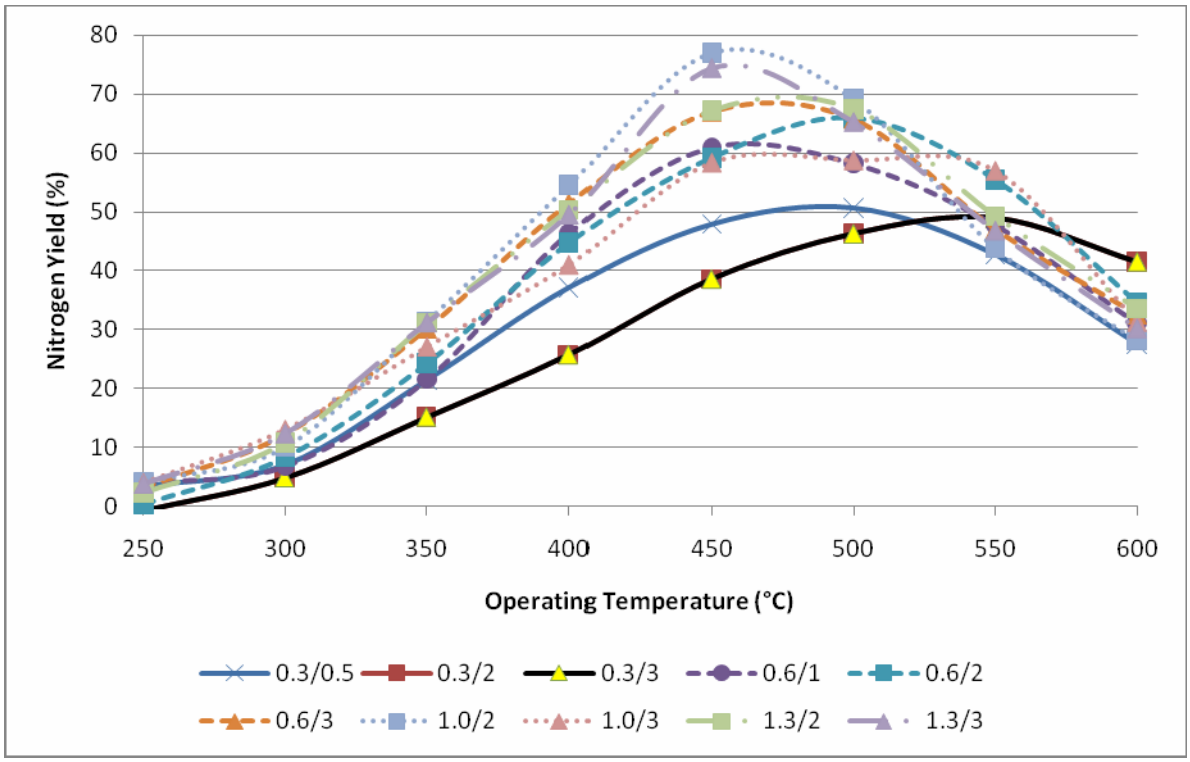

Figure 6: Nitrogen yield versus operating temperature for various levels of Pd/SZ. The first digit represents the alkoxide concentration [M] and the second the $Zr(OPr)_4/H_2SO_4$ ratio.

To determine the impact of the nominal sulfate ratio and $Zr(OPr)_4$ precursor concentration on nitrogen yield, a statistical analysis similar to the one done for surface area and pore volume was done on nitrogen activity. The factors studied were alkoxide concentration, $Zr(OPr)_4/H_2SO_4$ ratio, and operating temperature. The factor levels were again coded for better comparison with Equations (5) and (6) used to convert for alkoxide concentration and sulfate ratio, respectively, and Equation (9) used to convert between temperature and coded temperature.

$$T = \frac{Temperature - 425}{175} \qquad \text{Operating Temperature Conversion} \qquad \textbf{(9)}$$

Using the 12 unrejected catalyst samples, a regression model was developed that fit the data to a high degree of accuracy. The adjusted R^2 value was 0.964 out of 1.000. Replication of the data samples allowed for a maximum theoretical R^2_{max} value to be calculated, which was shown to be

0.995. Such a high R^2_{max}, incidcates that the nearly all effects were accounted for in the model (remember that palladium loading is constant in all samples). After checking for proper fit, a test of residuals and sample variability showed that the system contained two outliers. These outliers occurred at sample levels 1.0/2 and 1.3/3 at an operating temperature of 450°C. These outliers are interesting as the points correspond to the most and second most active points for nitrogen yield and the 1/2 levels corresponds to the standard sample. For the purposes of this report these points were assumed to be outliers and not used in the analysis, however, the 1.0/2 point has been reproduced and is probably a special operating point. This special outlier is also the sample that contained the most sulfur after calcination. The regression model is shown in Equation 10 with a list of values for the coefficients shown in Table 4. The model is lengthy and includes primarily interaction effects. This model is not to be taken as 'fundamental' formula for this system, but rather it is an empirical model that best fit the activity data.

$$\textbf{N}_2\textbf{ yield (\%)} = \beta o + \beta_1 T + \beta_2 T^2 + \beta_3 T^3 + \beta_4 T^4 + \beta_5 C^2 + \beta_6 C^2 S^2 + \beta_7 C^2 T^2 + \beta_8 C^3 + \beta_9 C^3 T^2 + \beta_{10} C^3 S + \beta_{11} C^2 T^2 S + \beta_{12} C^2 TS \quad \textbf{(10)}$$

Table 4: List of Coefficients for Equation (10)

βo	56.46	**β_4**	20.66	**β_8**	11.24
β_1	44.91	**β_5**	-10.96	**β_9**	-11.79
β_2	-60.42	**β_6**	10.54	**β_{10}**	-2.11
β_3	-28.80	**β_7**	14.90	**β_{11}**	-13.08
β_{12}	-2.89				

Equation 10 and Table 4 show that the primary effect, by far, is operating temperature. The model indicates that best fit includes a fourth degree effect for temperature and that a maxima is present in temperature's effect on activity. This temperature trend is expected and is well known. What is more challenging is diciphering the effects of $Zr(OPr)_4$ concentration and the nominal sulfate ratio on nitrogen yield. The model indicates that alkoxide concentrstion has the greatest impact after temperature and is shown in all interaction effects as well as an independent square and cubic form. The nominal sulfate ratio is the least important effect and is acting as an interaction effect only. To illustrate the effects of concentration and sulfate ratio, Figures 7,8, 9, and 10 show changes in factors and how they relate to nitrogen yield.

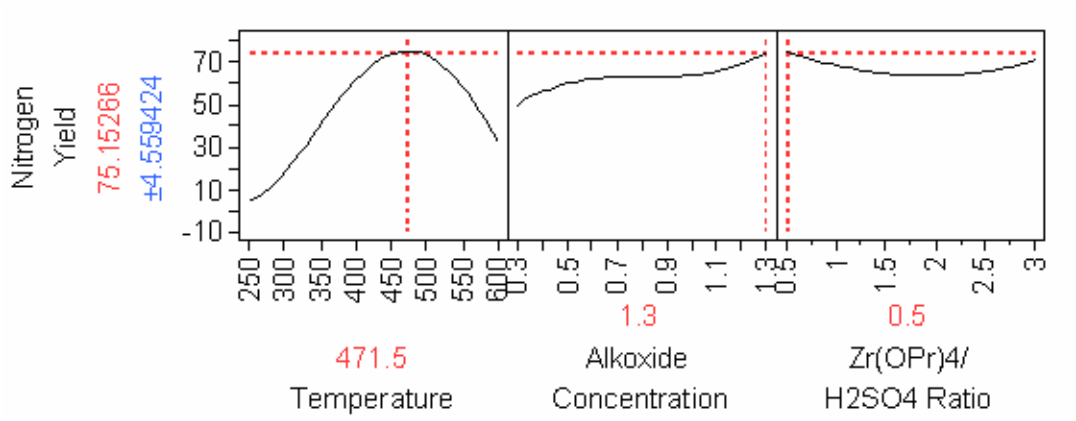

Figure 7: Optimized settings for nitrogen yield according to model. Temperature [=] °C, $Zr(OPr)_4$ Concentration [=] M

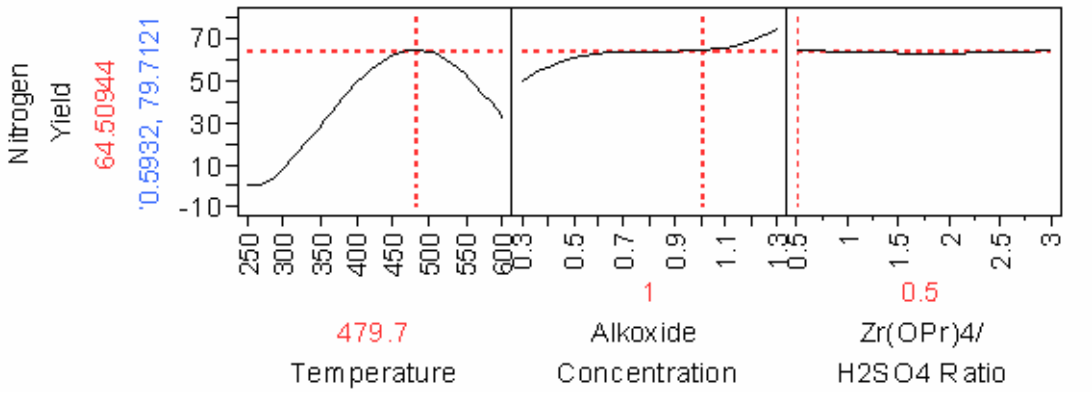

Figure 8: Maximum nitrogen yield when alkoxide concentration is 1 [M]. Effect of sulfate ratio is insignificant, optimized temperature increases.

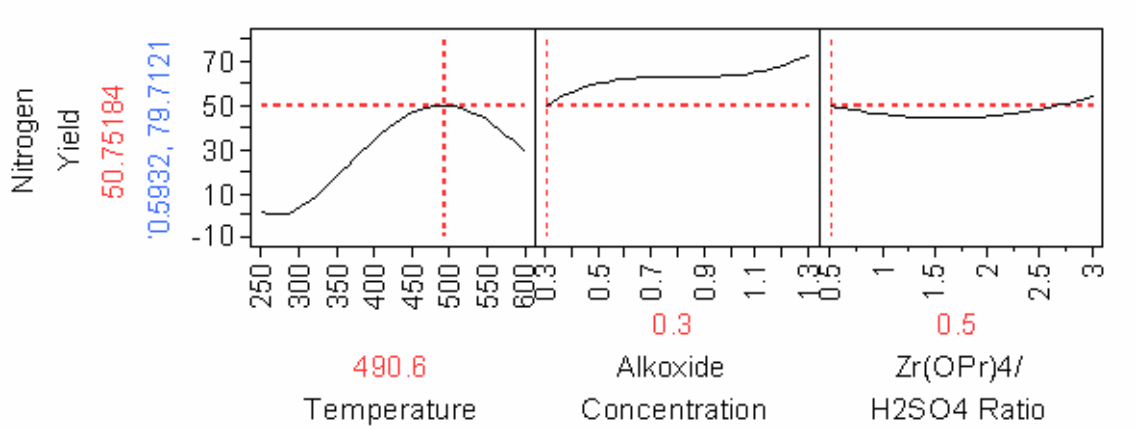

Figure 9: Maximum nitrogen yield when alkoxide concentration is 0.3 [M]. Effect of sulfate ratio restores to minimum trend, optimized temperature increases.

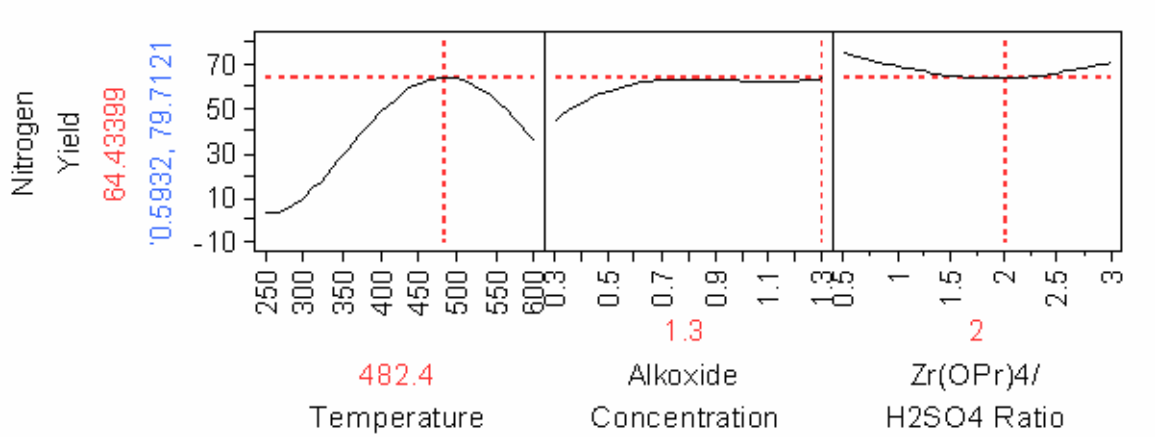

Figure 10: Maximum nitrogen yield obtained when sulfate ratio is increased from 0.5 to 2. High range of alkoxide concentration flattens, optimized temperature mildly increases.

Figure 7 optimizes the total model and estimates the factors that will lead to maximum yield. A maximum yield was estimated to be about 75.15 % when operating at a temperature of 471.5°C using 1.3 M $Zr(OPr)_4$ and a $Zr(OPr)_4/H_2SO_4$ ratio of 0.5. The sulfate ratio leans towards results seen in other preparation methods where a higher loading of sulfate equates to better activity. It is interesting to point out the presence of a minimum in the sulfate ratio around , which is in direct disagreement with experimental results. Again, the outlier is stting outside what the model predicts. In general, the model of the data shows there are significant interactions that occur so that neither sulfate ratio nor alkoxide concentration are independent of one another.

Figure 8 illustrates the interaction effects when the alkoxide concentration is reduced from 1.3 M to 1 M. Notice when that when the alkoxide concentration is decreased, the minimum found in the sulfate ratio flattens out so that no level of sulfate significantly impacts activity one way or the other. The sulfate ratio remains insignificant as $Zr(OPr)_4$ concentration continues to decrease until the minimum is restored around 0.7 M. Reducing the concentration lowers the overall nitrogen yield of the catalyst as shown in Figure 9. The $Zr(OPr)_4/H_2SO_4$ ratio also effects the alkoxide concentration effects. Starting from the settings in Figure 7, a decrease in the sulfate ratio towards the minimum (see Figure 10) tends to flatten the effects of alkoxide concentration at higher concentrations . The ideal operating temperature is also affected by the catalyst loadings. As alkoxide concentration decreased, the optimized operating temperature increased. This effect is also shown in Figure 6 where the nitrogen yield versus temperature chart had higher optimized operating temperatures for the 0.3/2 and 0.3/3 Pd/SZ samples. The sulfate ratio appears to increase the operating temperature when the ratio is at the minimum point. When the sulfate ratio has no effect on yield, due to the alkoxide concentration (~0.7 – 1.0 M), the temperature is not affected either.

Summarizing the activity of the catalysts through this regression model, one can conclude that operating temperature, alkoxide precursor concentration, and the nominal $Zr(OPr)_4/H_2SO_4$ ratio impact activity. Operating temperature is the dominant effect and tends to maximize nitrogen yield between 450 – 500°C. In addition, temperature tends to be affected by the alkoxide concentration and to a lesser extent the initial $Zr(OPr)_4/H_2SO_4$ ratio. Lower concentrations and sulfate ratios operating in its minimum range tend to increase the maximum nitrogen-yielding temperature. The $Zr(OPr)_4$ concentration tends to interact strongly with temperature and the sulfate ratio. Overall, the model predicts that better yields can be obtained when the concentration is 1.3 M and that a higher sulfate ratio of around 0.5 will give better yields, though a low ratio of 3 also improved yields, due to the minima seen in the sulfate ratio. In terms of the regression

model, the 1.3/3 palladium on sulfated zirconia sample performed the best, which it did when outliers were removed. But the model developed to reflect the data also indicates that higher activity could be obtained if the sulfate ratio were to be decreased beyond the minimum (higher loading of sulfate). The intereactions in this system seem to show dead zones for sulfate ratio effects around 0.7-1.0 M $Zr(OPr)_4$. The same could be said for the alkoxide concentration, when the sulfate ratio negated the effects of high concentration when operating around its minimum. Outside of the model predictions, the sample prepared with 1 M $Zr(OPr)_4$ and a sulfate ratio of 2 had the overall best yield. It is the sample that retained the most sulfur and does not fit with the model, which predicts a minimum to occur. This implies that the 1/2 catalyst may be a unique point, and should be studied more intensely with characterization techniques.

Linking Activity Results with Surface Area and Pore Volume Data

As a point of interest, the $Zr(OPr)_4$ concentrations and sulfate ratios used to obtain maximum surface area and pore volume were incorporated in the regression model of the activity data. Both results indicated that high surface area and pore volume do not necessarily equate to high activity. Using the 0.32 M $Zr(OPr)_4$ at a $Zr(OPr)_4/H_2SO_4$ ratio of 1.02 (maximum surface area) had a maximum yield operating temperature of about 498°C with a nitrogen yield of 47.9%. The pore volume fared slightly better with an operating temperature of 482°C with a nitrogen yield of 63.9%. It may be that the surface area only impacts the palladium dispersion and that for these Pd/SZ catalysts, the surface area, though not maximum, was already sufficient even at high sulfate ratios for effective palladium dispersion.

Effects of Using Pd-based Sulfated Ceria as an IWI Catalyst for NO_2 Reduction

Six palladium based, sulfated ceria catalysts were synthesized to test their potential in NO_2 reduction. The catalysts were prepared through incipient wetness impregation and doped with sulfur and palladium by using ammonium sulfate and palladium chloride, respectively in two

stages. The samples were calcined at 500°C and tested under the same conditions as those used in the Pd/SZ samples. Results for nitrogen yield were poor and no sample had any appreciable activity. The only results to report on was that there seemed to be significant partial reduction of NO_2 back to NO, which may be the same side reaction seen by the HCRG [34]. Work in this area is expected to continue by next using mixed palladium-based catalysts on ceria and sulfated zirconia supports and by making sol-gel ceria catalysts to see if these factors affect activity.

Conclusion

New formulations of sol-gel catalysts that varied alkoxide concentration and $Zr(OPr)_4/H_2SO_4$ ratio were active for NO_2 reduction across a continuum of ranges. According to the model, the sample prepared with 1.3 M $Zr(OPr)_4$ and a sulfate ratio of 3 performed the best, though the model predicts better performance could be obtained using a sulfate ratio of 0.5. The experimental data, however, showed that the catalyst with a 1.0 M alkoxide concentration with a sulfate ratio of 2 had the greatest activity though the regression model reported this as an outlier. While the value is an outlier, it is possibly significant as the activity was reproducible, coincides with the point of highest sulfur retention, and does not fit the prediction given in the model. In the sol-gel samples, temperature was the dominant effect, followed by alkoxide concentration, and finally the $Zr(OPr)_4/H_2SO_4$ ratio. Significant interactions occurred according to the model and a change in one parameter led to changes in other parameters. The Pd-based sulfated ceria catalysts were not active for NO_2 reduction with current formulations. More work is being done to use a mixed zirconia-ceria support as well as looking into sol-gel options for ceria. Statistical analysis of the results was effective in showing significance, detecting outliers, and giving insight into the next direction of formulations for further optimization.

References

[1] V.I. Pãrvulescu, P. Grange, B. Delmon Catalysis Today 46 (1998) 233- 316.
[2] R. Burch, Catalysis Reviews 46 (2004) 271-333.
[3] M.D. Amiridis, T. Zhang, R.J. Farrauto, Applied Catalysis B: Environmental 10 (1996) 203-227.
[4] J.J. A. Kubacka, E. Włoch, B. Sulikowski, Catalysis Today 101 (2005) 139-145.
[5] C. Loughran, D. Resasco, Applied Catalysis B: Environmental 5 (1994) 351-365.
[6] C. Loughran, D. Resasco, Applied Catalysis B: Environmental 7 (1995) 113-126.
[7] L.J. Lobree, A. W. Aylor, J.A. Reimer, A.T. Bell, Journal of Catalysis 181 (1998) 189-204.
[8] J.-Y. Yan, H. H. Kung,W. M. H. Sachtler, and M. C. Kung, Journal of Catalysis 175 (1998) 294-301.
[9] Y. Li, J. Armor, Journal of Catalysis 150 (1994) 376-387.
[10] Y. Li, P. Battavio, J. Armor, Journal of Catalysis 142 (1993) 561-571.
[11] R. Burch, J.P. Breen, F.C. Meunier, Applied Catalysis B: Environmental 39 (2002) 283-303.
[12] T. Komatsu, K. Tomokuni, I. Yamada, Catalysis Today 116 (2006) 344-249.
[13] M. Skoglundh, H. Johansson, L. Lijwendahl, K. Jansson, L. Dahl, B. Hirschauer, Applied Catalysis B: Environmental 7 (1996) 299-319.
[14] Y.-H. Chin, W. E. Alvarez, D. E. Resasco, Catalysis Today 62 (2000) 159-165.
[15] P. Vijayanand, K. Chakarova, K. Hadjiivanov, P. Lukinskasza and H. Knözingera, Physical Chemistry 5 (2003) 4040-4044.
[16] B.M. Reddy, P. M. Sreekanth, V. R. Reddy, Journal of Molecular Catalysis A: Chemical 225 (2005) 71-78.
[17] X. Song, A. Sayari, Catalysis Review - Sci. Eng. 38 (1996) 329-412.
[18] L.M. Kustov, V.B. Kazansky, F. Figueras, D. Tichit, Journal of Catalysis 150 (1994) 143-149.
[19] Y.-H. Chin, A. Pisanu, L. Serventi, W.E. Alvarez, D.E. Resasco, Catalysis Today 54 (1999) 419-429.
[20] P. Bautista, M. Faraldos, M. Yates, A. Bahamonde, Applied Catalysis B: Environmental 71 (2007).
[21] D. Farcasiu, J. Qi Li, S. Cameron, Applied Catalysis, A: General 154 (1997) 173-184.
[22] Q. Wu, H. Gao, and H. He, Journal of Physical Chemistry B 110 (2006) 8320-8324.
[23] T. Yamaguchi, T. Jin, and K. Tanabe, Journal of Physical Chemistry 90 (1985) 3148-3152.
[24] H. Armendariz, B. Coq, D. Tichit, R. Dutartre, and F. Figuéras, Journal of Catalysis 173 (1998) 345-354.
[25] D. Ward, E. Ko, Journal of Catalysis 157 (1995) 321-333.
[26] M.-T. Tran, N.S. Gnep, G. Szabo, M. Guisnet, Applied Catalysis A: General 171 (1998) 207-217.
[27] G. Karakas, J. Mitome-Watson, U.S. Ozkan, Catalysis Communications 3 (2002) 199–206.
[28] J.M. Watson, U.S. Ozkan, Journal of Catalysis 210 (2002) 295-312.
[29] N. Oktar, J. Mitome, E.M. Holmgreen, U.S. Ozkan, Journal of Molecular Catalysis A: Chemical 259 (2006) 171–182.
[30] J.M. Watson, U.S. Ozkan, Journal of Catalysis 217 (2003) 1–11.
[31] M.M. Yung, Oxidation Catalysis in Environmental Applications: Nitric Oxide and Carbon Monoxide Oxidation for the Reduction of Combustion Emissions and Purification of Hydrogen Streams, Chemical and Biomolecular Engineering, The Ohio State University, Columbus, 2007, p. 252.

[32] B.I. Gutiérrez-Ortiz, B. de Rivas, R. López-Fonseca, and J.R. González-Velasco, Journal of Thermal Analysis and Calorimetry 80 (2005) 225-228.
[33] Q. Liang, X. Wu, D. Weng, Z. Lu, Catalysis Communications 9 (2007) 202-206.
[34] E.M. Holmgreen, M.M. Yung, U.S. Ozkan, Catalysis Letters 111 (2006) 19-26.
[35] E.M. Holmgreen, M.M. Yung, U.S. Ozkan, Applied Catalysis B: Environmental 74 (2007) 73–82.
[36] E.M. Holmgreen, M.M. Yung, U.S. Ozkan, Journal of Molecular Catalysis A: Chemical 270 (2007) 101-111.

Appendix

Response Pore Volume
Summary of Fit

RSquare	0.968217
RSquare Adj	0.930078
Root Mean Square Error	0.026403
Mean of Response	0.196667
Observations (or Sum Wgts)	12

Analysis of Variance

Source	DF	Sum of Squares	Mean Square	F Ratio
Model	6	0.10618114	0.017697	25.3862
Error	5	0.00348552	0.000697	**Prob > F**
C. Total	11	0.10966667		0.0014*

Lack Of Fit

Source	DF	Sum of Squares	Mean Square	F Ratio
Lack Of Fit	4	0.00168552	0.000421	0.2341
Pure Error	1	0.00180000	0.001800	**Prob > F**
Total Error	5	0.00348552		0.8924
				Max RSq
				0.9836

Parameter Estimates

Term	Estimate	Std Error
Intercept	0.2763023	0.016686
Sulfate Ratio(0.5,3)	-0.231537	0.048795
Sulfate Ratio*Sulfate Ratio	-0.074368	0.02832
Sulfate Ratio*Sulfate Ratio*Sulfate Ratio	0.1598041	0.05001
Alkoxide Concentration(0.3,1.3)	-0.026918	0.017039
Alkoxide Concentration*Alkoxide Concentration	-0.05207	0.019281
Alkoxide Concentration*Sulfate Ratio	0.041485	0.025618

Residual by Predicted Plot

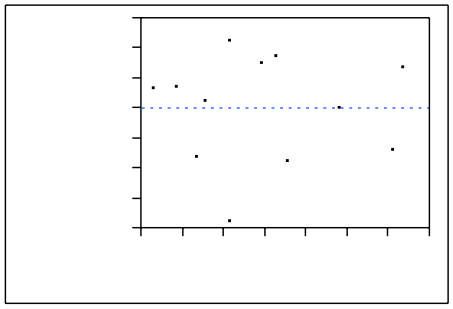

Activity Testing

Response Nitrogen Yield
Summary of Fit

RSquare	0.969042
RSquare Adj	0.964456

Root Mean Square Error	3.998205
Mean of Response	34.62372
Observations (or Sum Wgts)	94

Analysis of Variance

Source	DF	Sum of Squares	Mean Square	F Ratio
Model	12	40530.728	3377.56	211.2872
Error	81	1294.837	15.99	**Prob > F**
C. Total	93	41825.565		<.0001*

Lack Of Fit

Source	DF	Sum of Squares	Mean Square	F Ratio
Lack Of Fit	66	1103.5567	16.7206	1.3112
Pure Error	15	191.2801	12.7520	**Prob > F**
Total Error	81	1294.8368		0.2876
				Max RSq
				0.9954

Parameter Estimates

Term
Intercept
Temperature(250,600)
Temperature*Temperature
Temperature*Temperature*Temperature
Temperature*Temperature*Temperature*Temperature
Alkoxide Concentration*Alkoxide Concentration
Alkoxide Concentration*Alkoxide Concentration*Zr(OPr)4/H2SO4 Ratio*Zr(OPr)4/H2SO4 Ratio
Alkoxide Concentration*Alkoxide Concentration*Temperature*Temperature
Alkoxide Concentration*Alkoxide Concentration*Alkoxide Concentration
Alkoxide Concentration*Alkoxide Concentration*Alkoxide Concentration*Temperature*Temperature
Alkoxide Concentration*Alkoxide Concentration*Alkoxide Concentration*Zr(OPr)4/H2SO4 Ratio
Alkoxide Concentration*Alkoxide Concentration*Temperature*Temperature*Zr(OPr)4/H2SO4 Ratio*Zr(OPr)4/H2SO4 Ratio
Temperature*Alkoxide Concentration*Zr(OPr)4/H2SO4 Ratio*Zr(OPr)4/H2SO4 Ratio*Alkoxide Concentration

Prediction Profiler

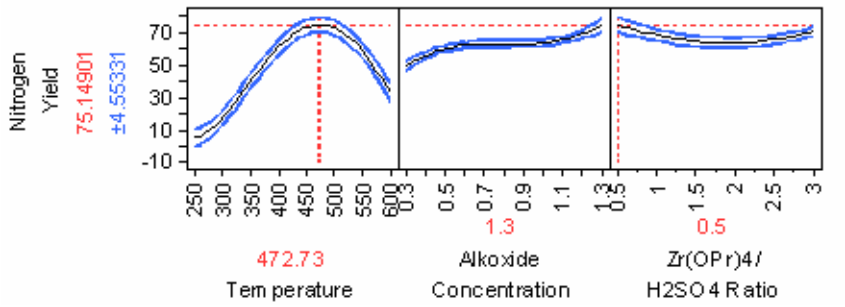

Distributions
Studentized Residuals for Nitrogen Yield

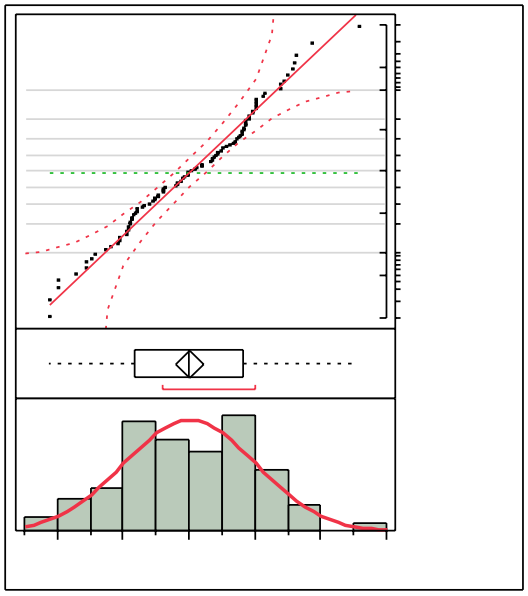

Normal(0.00093,1.005)

Quantiles

100.0%	maximum	2.583
99.5%		2.583
97.5%		1.761
90.0%		1.248
75.0%	quartile	0.817
50.0%	median	0.00734
25.0%	quartile	-0.832
10.0%		-1.366
2.5%		-2.077
0.5%		-2.130
0.0%	minimum	-2.130

Moments

Mean	0.0009321
Std Dev	1.0049967
Std Err Mean	0.1036575
Upper 95% Mean	0.2067753
Lower 95% Mean	-0.204911
N	94

Fitted Normal
Parameter Estimates

Type	Parameter	Estimate	Lower 95%	Upper 95%
Location	μ	0.0009321	-0.204911	0.2067753
Dispersion	σ	1.0049967	0.8790028	1.1734868

-2log(Likelihood) = 266.697493253211

Goodness-of-Fit Test

Shapiro-Wilk W Test

W	Prob<W
0.983093	0.2665

Note: Ho = The data is from the Normal distribution. Small p-values reject Ho.